# EVALUATION METHOD OF DAMPING RATIO USING EARTHQUAKE RECORDS AND ITS APPLICATION IN DAM ENGINEERING

Z. Cao(1), M. Kashiwayanagi(2), M. Yoshida(3), H. Asaka(4),

(1) *Senior Engineer, Social & Envir. Eng. Dept., J-POWER Business Service Corporation, sou@jpbs.co.jp*
(2) *Senior Advisor, Chigasaki Research Institute, J-POWER, masayuki_kashiwayanagi@jpower.co.jp*
(3) *Director, Lease Business Dept., J-POWER Business Service Corporation, Masatoshi_yoshida@jpbs.co.jp*
(4) *Deputy Director, Social & Envir. Eng. Dept., J-POWER Business Service Corporation, Asaka@jpbs.co.jp*

## *Abstract*

A method for evaluating damping ratio of structures using earthquake records is developed in this study. In the proposed method, the wave after the peak value of the earthquake record obtained at the top of the structure is decomposed in to free vibration component and forced vibration component. Logarithmic Decrement Method is applied to the obtained free vibration to find the damping ratio of the structure. The forced vibration is obtained by multiplying the transfer function matrix [1] based on the past three sets of earthquake records by the Fourier spectra of the input ground motions and inversely Fourier transformation (FFT). The validity of the proposed method is verified by comparing the results of the dynamic FEM analysis of a structural model and the results evaluated by this method. However, it is sometimes difficult to get an ideal free vibration in the cases of real dams since the response at the top of a dam is not just a function of the ground motion at the dam base. The applicability of the proposed method in real dams is studied. The damping ratio of a concrete gravity dam was evaluated using 15 sets of earthquake records. It is found that the damping ratio of the dam is 2 - 6% with no obvious dependence on the peak ground acceleration when it is under 50 cm/s$^2$. The contribution of reservoir water to damping ratio is estimated to be approximately 1% when water depth increases from 60 m to 100 m. It is concluded that the proposed method is practical for evaluating the damping ratio of dams.

*Keywords: damping ratio, earthquake record, dam, evaluation method, Logarithmic Decrement Method*

## 1. Introduction

Damping ratio is one of the very important parameters in seismic response analysis and seismic safety evaluation of structures. Damping in structures can be classified into those due to structural reasons and material reasons according to the mechanism of their occurrence. In seismic response analysis of structures, structural damping and material damping are generally set as a constant. In addition, for simulating the dissipation of energy from the structure to the ground or from the foundation ground to the infinite natural ground, the dissipation attenuation must also be considered. For this reason, it is practically difficult to evaluate the damping of structures existing in nature quantitatively and accurately.

In dam engineering, many studies have been done on damping evaluation. Matsumoto et al. [2] measured material damping due to non-linearity of coarse-grained materials through material tests. Ueda et al. [3] investigated the relationship between damping ratios and vibration amplitudes of two arch dams based on vibration tests and earthquake records. Sato et al. [4] estimated the dynamic and physical properties of an existing dam based on earthquake records. It is often reported that damping ratios are identified by reproduction analysis of the seismic behavior of dams [5], [6]. However, the accuracy of the damping ratio evaluation result is not sufficient due to various restrictions.

In the field of civil engineering and construction, two methods are mainly used to estimate the damping ratio of structures using seismic records and experimental results. One is to calculate the damping ratio by the half-power method [7] with the frequency response function obtained from earthquake records, as shown in

Fig. 1. In the half-power method, the frequency corresponding to the maximum amplitude $A$ is marked as $f_0$. The frequencies $f_1$ and $f_2$ are those corresponding to the amplitudes of $A/\sqrt{2}$ of the frequency response function. Hence, a damping ratio can be obtained from the equation $h = (f_2-f_1) / (2f_0)$. However, the frequency response function obtained from seismic records is not generally smooth, and it is necessary to smooth the frequency response function before applying the half-power method. As shown in Fig. 1, as the number of smoothing increases, the frequency response function becomes smoother, but the error of the calculated damping ratio increases. Another is the Logarithmic Decrement Method (referred to as LDM) [8], which is calculated by Eq. (1) based on the change in the amplitude of the free vibration, as shown in Fig. 2, of a structure. However, it is extremely difficult to excite the free vibration of a large structure such as a dam or a bridge without a special large seismic equipment.

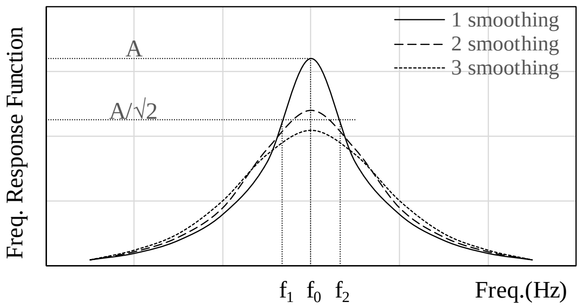


Fig. 1 - Half-Power Method

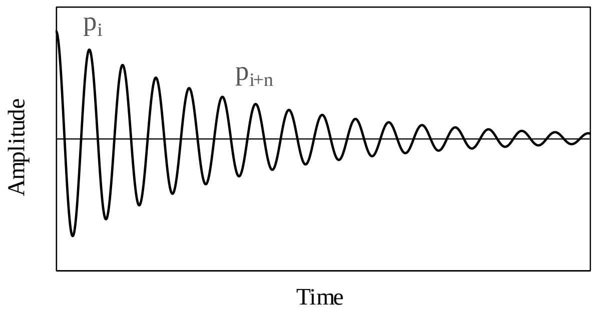


Fig. 2 - Logarithmic Decrement Method

$$h = \frac{1}{2\pi n} \ln\left(\frac{p_i}{p_{i+n}}\right) \tag{1}$$

The study is to propose a method for evaluating the damping ratio of structures. In the method, the seismic records of structures are decomposed into forced vibrations and free vibrations, and the LDM is applied to the free vibration to accurately calculate the damping ratio of structures existing in the natural environment. For verification of the method, the free vibration of a assumed model is analyzed by the conventional FEM analysis, and compared with the calculation results of the proposed method. Furthermore, application of the proposed method to an existing dam was examined. The practicality and validity of the proposed method are confirmed by applying the proposed method to a concrete arch dam with 15 sets of earthquake records.

## 2. Calculation method of damping ratio using earthquake records

### 2.1 Outline of the proposed method

The proposed method decomposes the earthquake record of a structure in to forced and free vibrations and calculates the damping ratio of the structure by applying the Logarithmic Decrement Method to the obtained free vibration. The proposed method is described below with emphasis on the method of obtaining the forced vibration.

It is assumed that there are three-directional earthquake records $A$ and $B$ at the top $a$ and foundation $b$ of the structure, as shown in Fig. 3. For simplicity, Fig. 4 shows only 1-directional component of an earthquake record as an example. These earthquake records are divided into two time-zones before and after the time of occurrence of the maximum acceleration value at the top. As shown in Fig. 4, these waves are called $A_1$ and $A_2$ at the top and $B_1$ and $B_2$ at the foundation. Considering the propagation time $\Delta t$ of the wave from the foundation to the top, strictly speaking, the start times of $B_2$ and $A_2$ are different. But here, it is supposed that $A_2$ and $B_2$ start simultaneously. The response $A_2$ at the top is considered to be the combination of the free vibration $F_2$ of the structure excited by the input ground motion $B_1$ and the forced vibration $R_2$ due to the input ground motion $B_2$. If the forced vibration $R_2$ can be accurately obtained by an appropriate method, the free vibration $F_2$ at the top can be obtained by excluding $R_2$ from $A_2$. That is,

$$F_2 = A_2 - R_2 \tag{2}$$

Then, the damping ratio of the structure can be obtained when the Logarithmic Decrement Method (Eq. (1)) is applied to the free vibration $F_2$. Therefore, the fundamental problem of our proposed method is how to find the forced vibration $R_2$ with high accuracy.

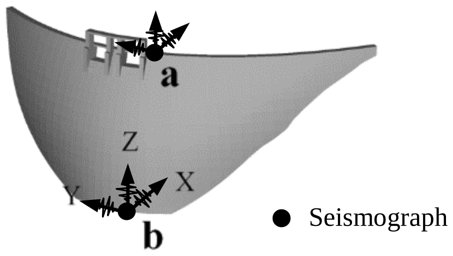


Fig. 3 - Earthquake monitoring image

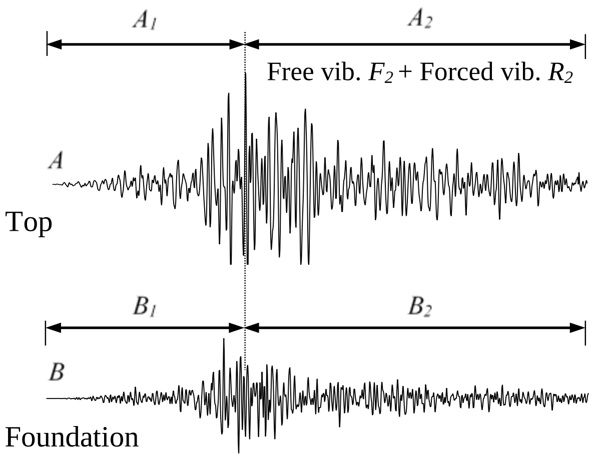


Fig. 4 – Example of earthquake record

## 2.2 Calculation of forced vibration $R_2$

First, to calculate the forced vibration $R_2$, the following transfer function matrix [T] is obtained using three sets of past earthquake records [1].

$$[T] = \begin{bmatrix} T_{xx} & T_{xy} & T_{xz} \\ T_{yx} & T_{yy} & T_{yz} \\ T_{zx} & T_{zy} & T_{zz} \end{bmatrix} \tag{2}$$

where, each component $T_{ij}$ $(i, j = X, Y, Z)$ of the matrix is a transfer function that considers mutual interference between directions. In Fig. 3, $T_{ii}$ $(i = X, Y, Z)$ is the transfer function showing the response characteristics in the $i$ direction at point $a$ to the vibration in the $i$ direction at point $b$ of the structure. Each component $T_{ij}$ $(i, j = X, Y, Z$, but $i \neq j)$ is a contribution transfer function introduced to consider mutual interference between directions. For example, $T_{xy}$ shows the response characteristics in the $X$ direction at point $a$ to the vibration in the $Y$ direction at point $b$. Details of how to calculate the transfer function matrix are given in related reference [1].

Using $[T]$ and the Fourier spectrum $\{S_i^{B_2}\}$ $(i = X, Y, Z)$ of the input ground motion $B_2$ at the foundation $b$ (the time history is shown in Fig. 5) of the structure, the Fourier spectrum $\{S_i^{R_2}\}$ $(i = X, Y, Z)$ of the forced vibration in the same time region at the top a of the structure is obtained as shown in Eq. (3).



 

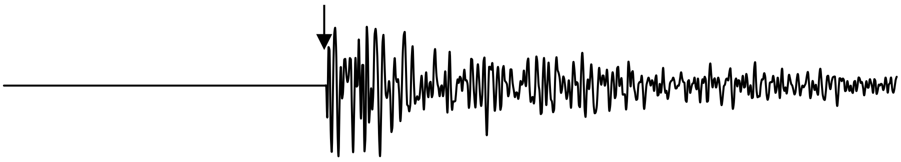


Fig. 5 - Input wave $B_2$

$$\{S_i^{R_2}\} = [T]\{S_i^{B_2}\} \ (i = X, Y, Z) \tag{3}$$

Each variable in Eq. (3) is a function of angular frequency, and Eq. (3) holds for each frequency. In this paper, for simplicity of description, the expression of angular frequency is omitted.

By inversing Fourier transformation of the $\{S_i^{R_2}\}$ obtained from Eq. (3), the forced vibration $R_2$ due to the input ground motion $B_2$ can be obtained. In addition, to obtain a free vibration with higher accuracy, it is better to cut high frequency components sufficiently separated from the primary natural frequency of the structure in each vibration direction. For example, in the case of a structure with a natural frequency of 5 Hz, cutting off the components with a frequency of 8 Hz or more will give a clear free vibration waveform. Since the contribution of the three directional components of the input earthquake motion are included in the method shown in Eq. (3), a high accurate $R_2$ can be obtained.

## 3. Verification analysis

### 3.1 Method of Verification

The analysis and comparison shown in Fig. 6 are performed to verify the validity of the proposed method. The calculated free vibration and damping ratio will be confirmed here. To obtain a clear conclusion, “artificial earthquake record " will be created instead of an actual earthquake record. The artificial earthquake record is obtained from the input wave and the response wave by performing an earthquake response analysis using the verification model. The transfer function matrix [$T$] of the model is obtained first using the 3 sets of artificial earthquake records. Then, the free vibration of the verification model is obtained for each of the records by Eq. (3). At the same time, the input waves used to create the above mentioned artificial earthquake records are inputted to the verification model until the time when the maximum acceleration values at the top of the model occurred. Then, the free vibrations are calculated by the direct integration method. The validity of the proposed method is confirmed by comparing the free vibrations obtained by the above two methods. In addition, the damping ratio of the verification model is obtained by the Logarithmic Decrement Method and compared with that used in the response analysis of the above model.

### 3.2 Verification conditions

An asymmetric verification model shown in Fig. 8 is used so that the artificial earthquake records obtained by the analysis have three dimensionalities. This model is assumed to be of linear material with the properties shown in Table 1. Regarding the damping in the response analysis, it is assumed to be proportional to the mass [M] and the rigidity [K] in the form [C] = α [M] + β [K], and the parameters α and β are set by Eq. (4).

$$\alpha = 1.4\omega_1 h \qquad \beta = 0.6h/\omega_1 \tag{4}$$

where, $\omega_1$ is the fundamental circular frequency of the verification model, and $h$ is the damping ratio shown in Table 1. The eigenvalue analysis performed prior to the earthquake response analysis shows that the fundamental eigenfrequency of the verification model is 7.12 Hz, which results in $\omega_1=2\pi f_1$=44.74.



 

Earthquake records of a real structure are used as the input ground motion in the analysis. Figure 9 shows one of the three sets of ground motions as an example. The response analyses are performed with the three-dimensional analysis program "UNIVERSE" [4], where direct integration method is used.

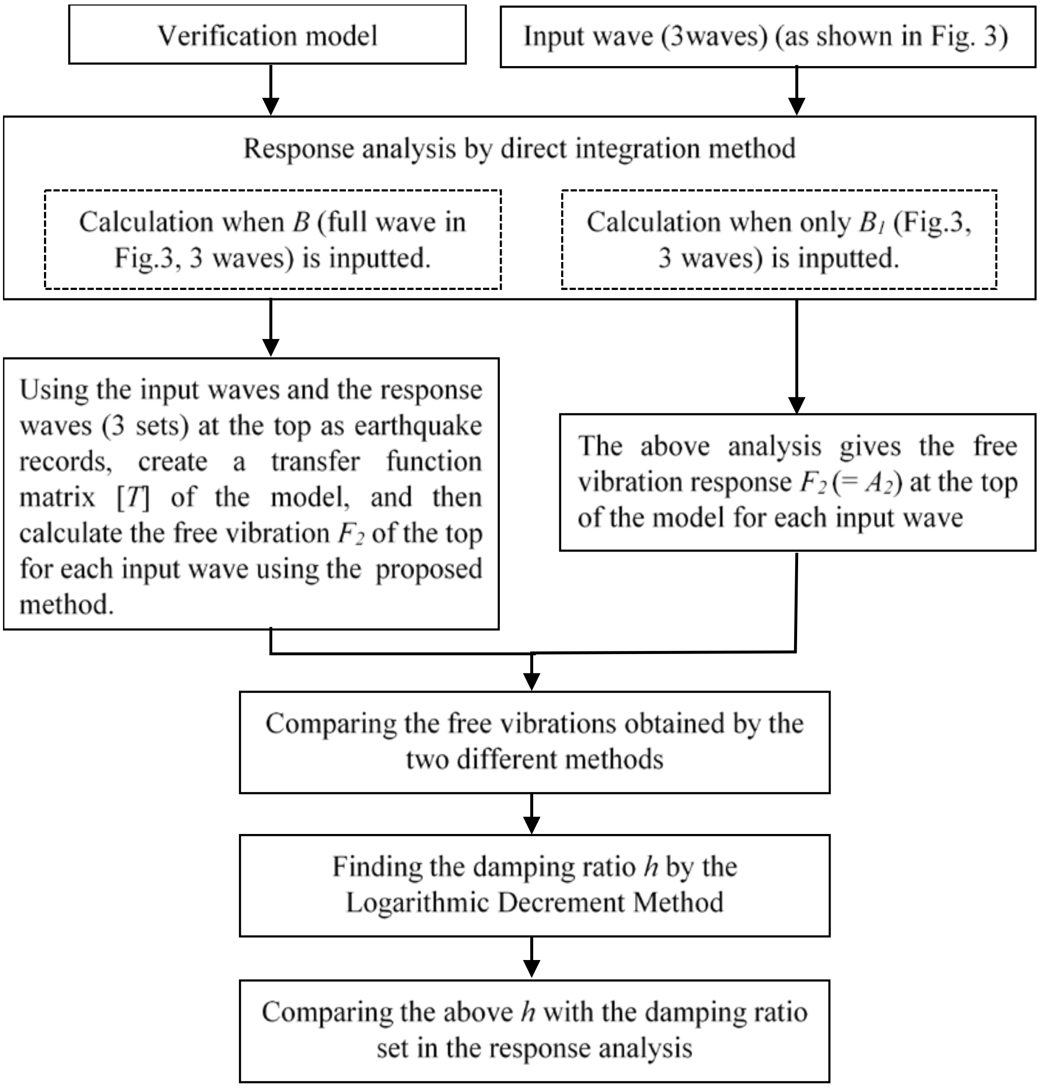


Fig. 6 - Flow of verification analysis

### 3.3 Verification results

By response analysis for three sets of input waves, the acceleration response histories at the bottom and top of the model shown in Fig. 8 were obtained as "artificial earthquake records". The waveforms of these outputs are not shown here. Using the three sets of artificial earthquake records, the transfer functions (shown in Fig. 10) of the model were obtained by the transfer function matrix method [1]. This figure shows the natural frequency of the model in three directions and the mutual interference between the directions of vibration. For example, since $T_{xy}$, $T_{xz}$, $T_{yx}$, and $T_{zx}$ are small, it is considered that mutual interference between the $X$ direction and the other two directions is relatively small. By multiplying this transfer function matrix [$T$] by the Fourier spectrum of the input wave $B_2$ (see Fig. 5) as in Eq. (3), the Fourier spectrum of the forced vibration $R_2$ of the model for each input wave is obtained. And the time history of forced vibration $R_2$ was obtained by inversing



 

Fourier transform. Furthermore, the acceleration time history at the top of the model when the model vibrates freely is calculated by Eq. (2). To obtain a clear free vibration, the components above 10 Hz were cut off.

Simultaneously with the above calculation, as shown in the flow on the right side of Fig. 6, the free vibration of the model is calculated with direct integration method. The model is excited with each input wave at the bottom of the model until the time when the maximum value of the acceleration response at the top is generated. Then the excitation is set to be zero (as shown in Fig. 7), and the calculation continues till the end of the original input wave.

Table 1 – Properties of verification model

| | |
|---|---|
| Shear modulus | 10000 N/mm$^2$ |
| Density | 2.4 g/cm$^3$ |
| Poisson's ratio | 0.2 |
| Damping ratio | 4.0% |

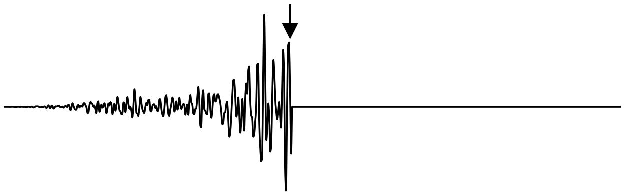


Fig. 7 - Input wave $B_1$

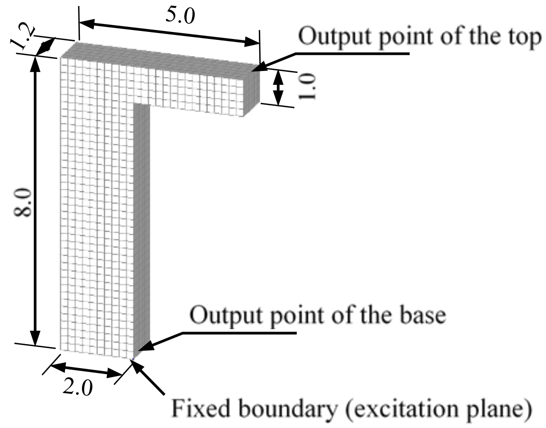


Fig. 8 - Model used for verification

The time histories of the free vibration at the top of the model obtained by the above two methods are compared. Here, only the vibration component in the $X$ direction is shown in Fig. 11 as an example. From Fig. 11, it can be found that the time history of the free vibration obtained by the proposed method well coincides with the result of the direct integration method for each input wave.

Using the peak values $P_1$ and $P_6$ in the free vibration shown in Fig. 11, the damping ratio of the model was calculated by the Logarithmic Decrement Method shown in Eq. (1). When calculating the free vibration, the excitation wave suddenly becomes zero at the time of the maximum value at the top, and the free vibration calculation immediately after may be unstable. Therefore, the time history of the free vibration used in the calculation starts from the second peak (see Fig. 11). Table 2 summarizes the damping ratios calculated. On the other hand, the damping ratio set in the response analysis performed to create the artificial earthquake record was 4%, so the maximum relative error of the calculation result of the proposed method was 5% compared to the actual setting value. It is clear the method has good accuracy.

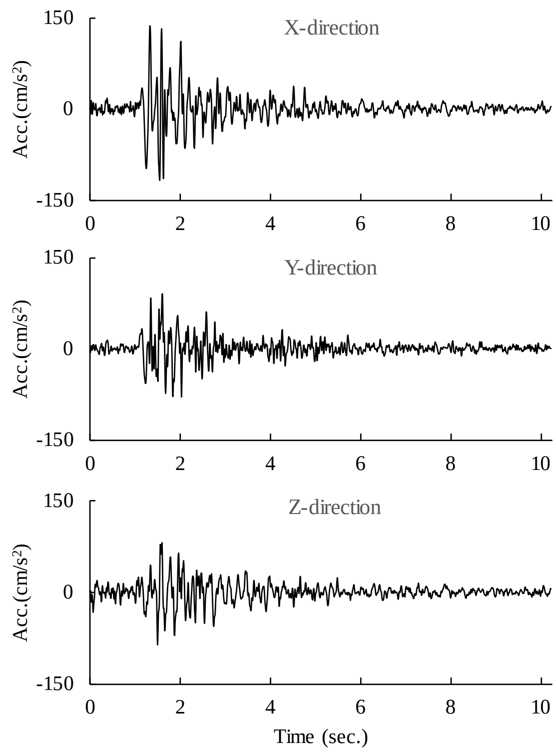


Fig. 9 - Example of input wave

Table 2 - Damping ratio obtained by the proposed method

| Input wave (Fig.11) | Proposed method | Set value in response analysis |
|---|---|---|
| 1 | 4.20% | |
| 2 | 4.04% | 4.00% |
| 3 | 4.17% | |

From the above verification analysis, it can be found that the free vibration of the model obtained by the proposed method well coincides with the result of the free vibration calculated by the conventional numerical analysis method. In addition, the evaluation result on the damping ratio of the model agrees with the value set in the model. Therefore, it is clear the proposed method can evaluate the damping ratio of structures based on earthquake records.

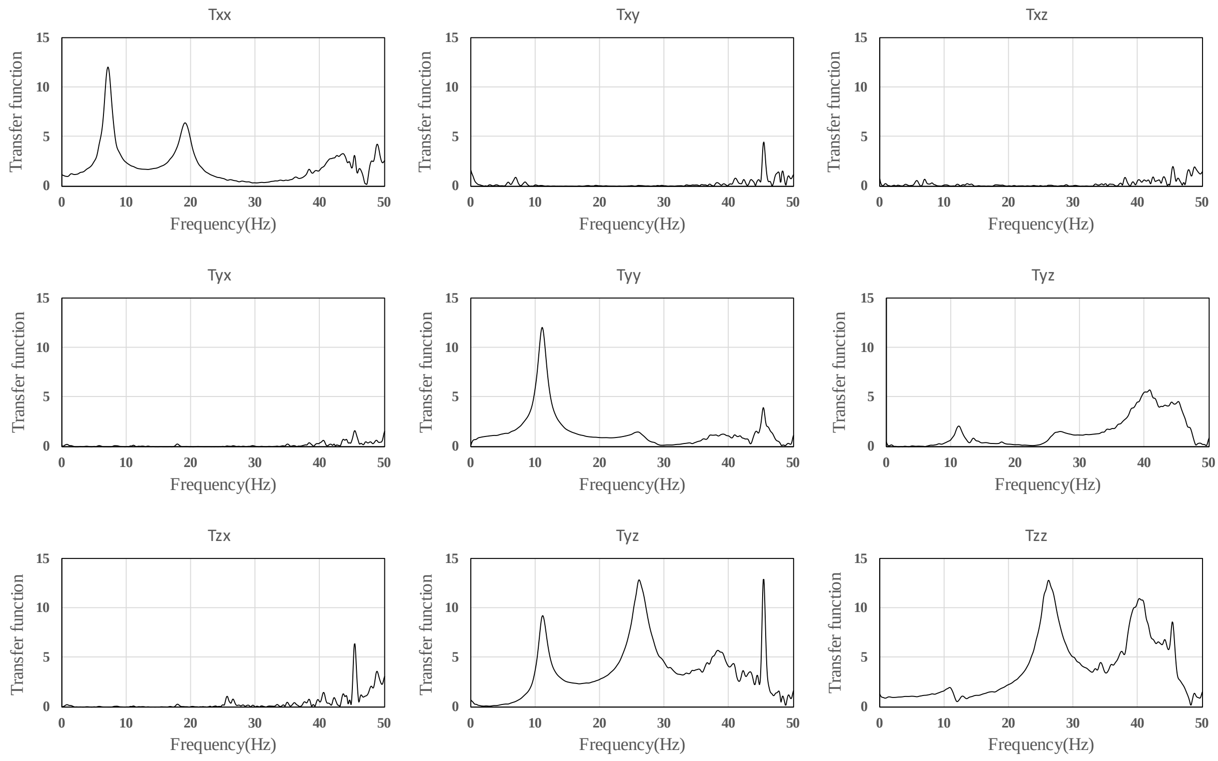


Fig. 10 - Transfer function matrix of the model for verification

## 4. Application in dam engineering

Dams are usually constructed on rocks of various shapes and geological conditions. Therefore, they show strong three-dimensional behaviors during earthquakes. Since the water level of the reservoir fluctuates year-round, the effect of dam-water interaction, the effect of temperature changes, the effect of non-linearity of embankment material in fill dams, and the non-linear behavior of arch dams due to the opening and closing of vertical joints, it is considered that the natural frequency and damping ratio of dams fluctuate in a complicated manner. When the proposed method is applied to a dam, three sets of earthquake records used to calculate the transfer function matrix and those used to calculate the damping ratio are selected in consideration of the following points.

1) The amplitudes of the seismic acceleration of the foundation are as close as possible.
2) The water levels at the time of the earthquake should not be much different.
3) The temperatures at the time of the earthquake are as close as possible.
4) The lengths of the earthquake records must be the same.



 

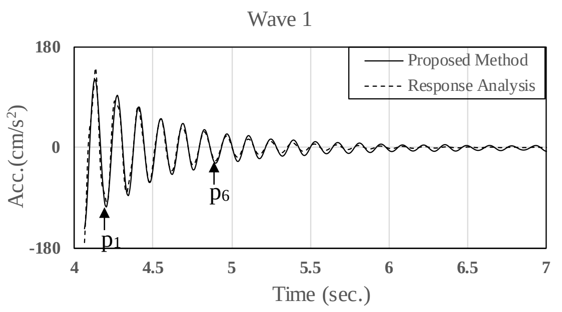


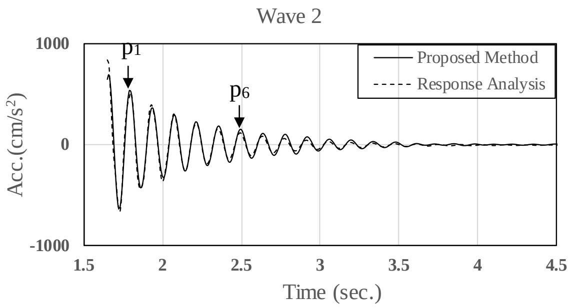


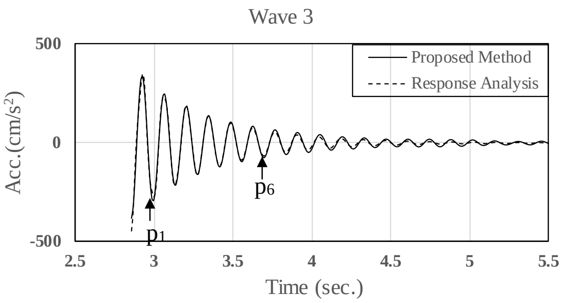


Fig. 11 - Comparison of the free vibration obtained by the proposed method and response analysis

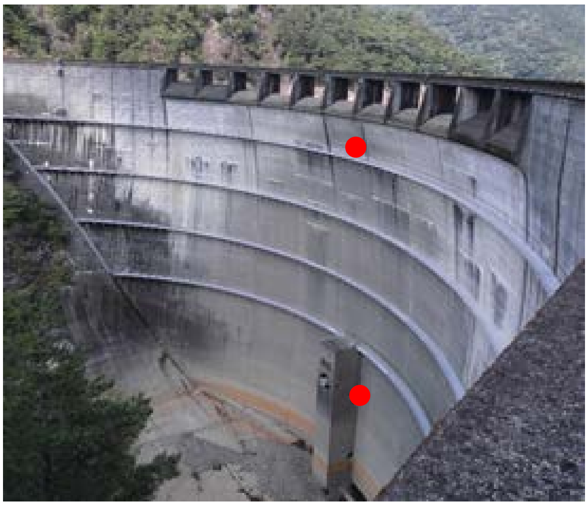

● Seismograph

Fig. 12 - Downstream surface of Sakamoto Dam and seismograph position

### 4.1 Object of the case study

Sakamoto Dam is a concrete arch dam with a height of 103 m and a crest length of 256.3 m. It is constructed in a relatively narrow valley. Figure 12 shows the downstream surface of the dam and the location of the seismographs. 15 earthquake records are extracted from the earthquake records recorded so far, and they are shown in Table 3 in the order of earthquake occurrence time. After calculating the transfer function matrix from these earthquake records, the damping ratio of the dam was estimated.

Table 3 – Earthquake records used in analysis

| No | Time of occurrence | Peak acc. (cm/s$^2$) | Damping ratio |
|---|---|---|---|
| 1 | 2007.04.15 12:19 | 12 | 3.12 |
| 2 | 2007.07.16 17:24 | 21 | 3.76 |
| 3 | 2008.11.10 10:31 | 4 | 4.26 |
| 4 | 2009.11.22 21:08 | 12 | 2.58 |
| 5 | 2010.04.12 09:01 | 8 | 3.01 |
| 6 | 2010.07.21 06:19 | 8 | 2.43 |
| 7 | 2011.07.05 19:18 | 9 | 3.24 |
| 8 | 2011.07.24 23:32 | 52 | 4.79 |
| 9 | 2011.09.16 07:15 | 9 | 4.25 |
| 10 | 2013.04.13 05:33 | 9 | 2.63 |
| 11 | 2014.02.19 01:50 | 7 | 5.52 |
| 12 | 2016.04.01 11:39 | 9 | 6.09 |
| 13 | 2017.09.17 08:28 | 4 | 2.86 |
| 14 | 2018.06.18 07:58 | 15 | 1.79 |
| 15 | 2018.11.02 16:54 | 8 | 2.66 |



 

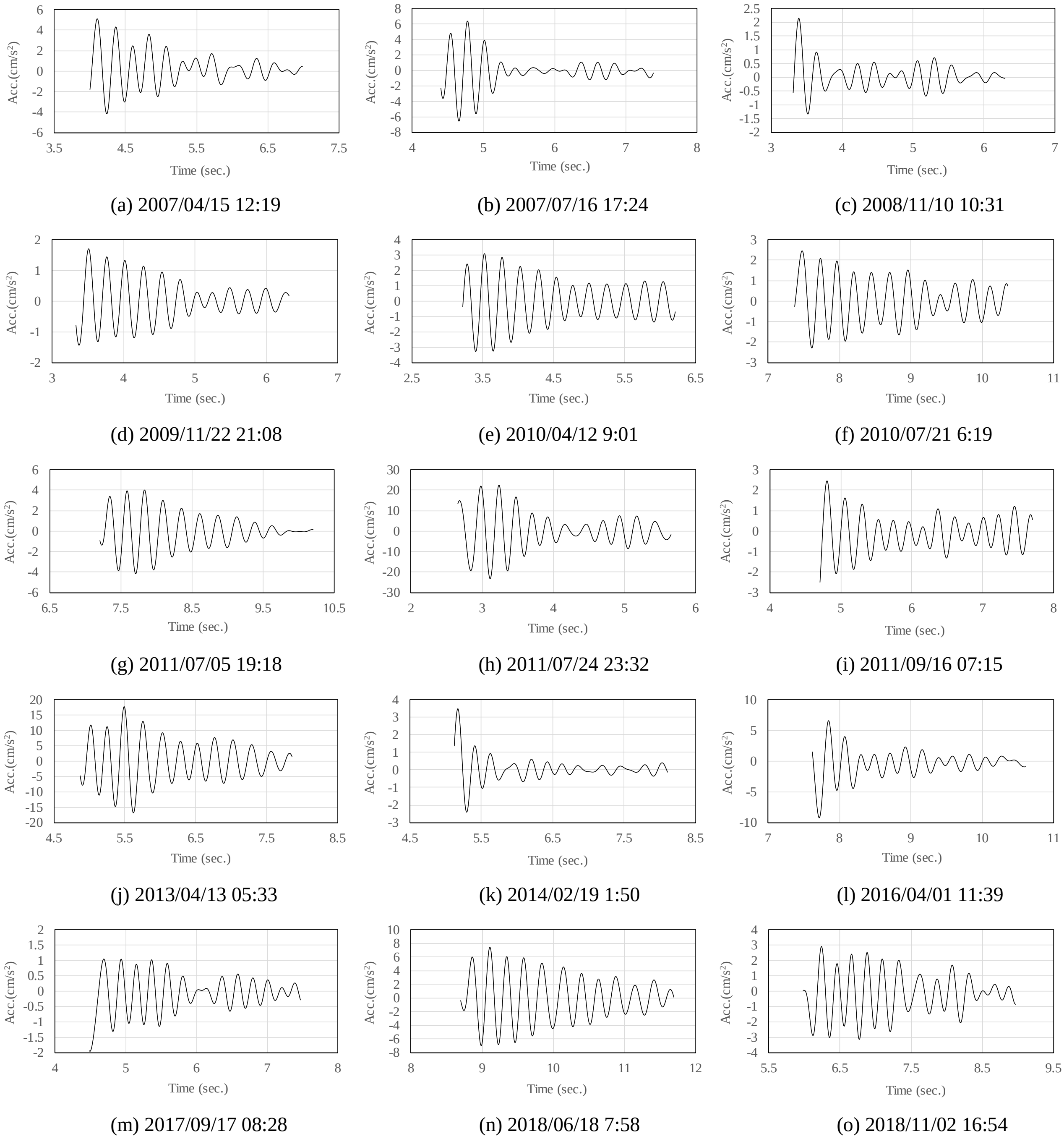


(a) 2007/04/15 12:19
(b) 2007/07/16 17:24
(c) 2008/11/10 10:31
(d) 2009/11/22 21:08
(e) 2010/04/12 9:01
(f) 2010/07/21 6:19
(g) 2011/07/05 19:18
(h) 2011/07/24 23:32
(i) 2011/09/16 07:15
(j) 2013/04/13 05:33
(k) 2014/02/19 1:50
(l) 2016/04/01 11:39
(m) 2017/09/17 08:28
(n) 2018/06/18 7:58
(o) 2018/11/02 16:54

Fig. 13 - Free vibration obtained by the proposed method
(after the peak acceleration of each earthquake record)

## 4.2 Evaluation method of damping ratio for real dams

Figure 13 shows the free vibrations obtained by the proposed method. They are corresponding to the parts after the peak values of the earthquake records at the upper seismograph of the dam. In order to have sufficient free vibration time and to make it easier to examine, the waves for 3 seconds after the peak values are extracted as



 

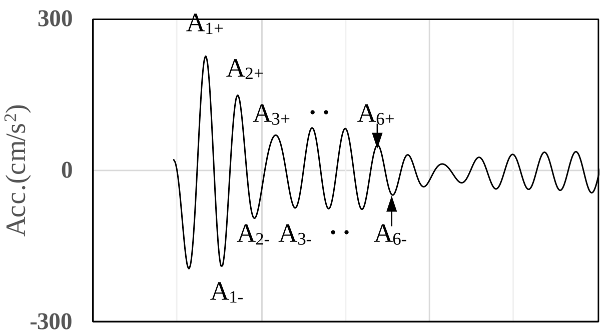


Fig. 14 – Example of the waveform obtained as free vibration of an existing dam

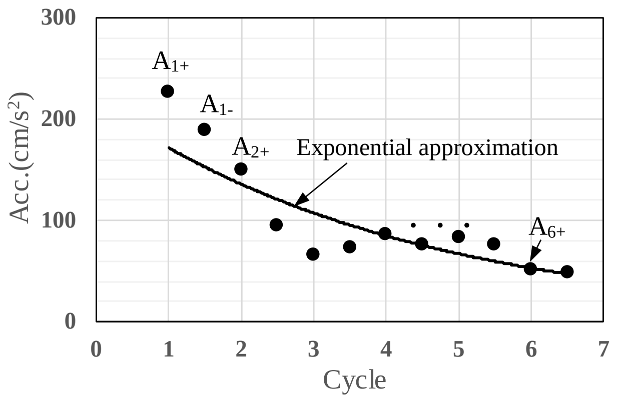


Fig. 15 - Exponential approximation

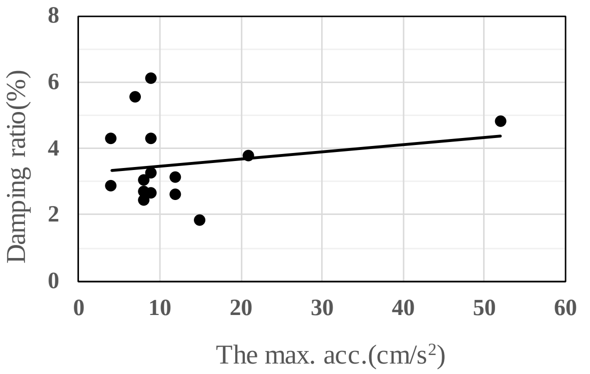


Fig. 16 - Relationship of peak acc. & damping ratio

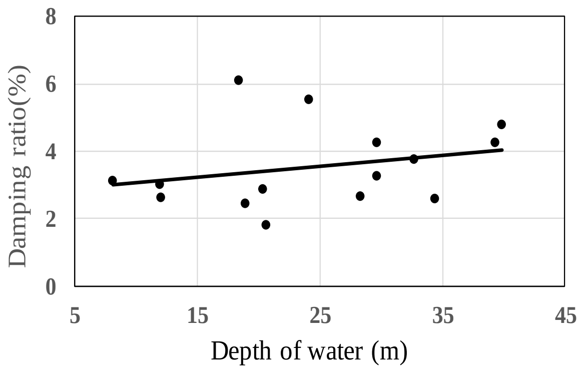


Fig. 17 - Relationship of water depth & damping ratio

shown in Fig. 13. LDM can be applied to about half of the waveforms. However, nearly half of the waveforms are far from ideal free vibrations, and it is difficult to apply LDM to some waveforms, for example, 2008/11/10 10:31 earthquake or 2014/2/19 1:50 earthquake etc. The accuracy of the calculation result (Fig. 11) is lower than that of the verification model shown in Fig. 8. In the verification model shown in Fig. 8, the input and the output of the vibration is in a clear one-to-one correlation, whereas in actual dams, the seismic response at the upper part of the dam is not only due to the ground motion at the lower part of the dam, but also due to the ground motion propagating through an arbitrary position on the abutment [10]. In addition, it is considered that the influence of the hydrodynamic pressure of the reservoir water and its reflection complicate the earthquake response of the dam. When the waveform of free vibration shown in Fig. 14 is obtained, it is difficult to find the damping ratio accurately. Therefore, the following approximation processing is performed on the waveform shown in Fig. 14 before applying the Logarithmic Decrement Method to it.

The peak values of the positive half amplitude of the waveform shown in Fig. 14 are denoted as $A_{1+}$, $A_{2+}$, etc. Similarly, those of the negative half amplitude are denoted to be $A_{1-}$, $A_{2-}$, and so on. Plotting the absolute peak values and the corresponding cycle numbers gives the relationship between the amplitude and the cycle number indicated by ● in Fig. 15. Furthermore, an exponential approximation curve is taken for this relationship. Instead of the original data, the damping ratio of the dam is determined by applying LDM (Eq. (1)) to this exponential approximation curve. Here, it is desirable that the exponential approximation process has peak values of at least three cycles.



 

### 4.3 Evaluation results

The damping ratio of Sakamoto Dam was calculated by the proposed method for the 15 earthquake records shown in Table 3, and the results are shown in the same table. Figure 16 shows the relationship between the estimated damping ratio and the maximum acceleration of the lower seismograph. As shown in Fig. 16, the calculated damping ratio of the dam varies from 2 to 6% when the maximum acceleration at the lower seismograph is less than about 50 $cm/s^2$. There are few seismic records of 20 $cm/s^2$ or larger at the lower seismograph, so that no clear relationship between damping ratio and acceleration amplitude can be obtained. However, an approximate line for this relationship is plotted in Fig. 16 for reference. This result was obtained based on earthquake records at the lower and upper parts of the dam (Fig. 12) and is considered to include the loss of vibration energy due to reservoir water. The relationship shown in Fig. 17 is obtained when the calculated damping ratio and the water depth of the reservoir at the time of each earthquake occurrence is plotted. Although there is a similar variation, the approximate line is added in the figure because the data at each water depth distribute approximately evenly. The figure shows that the damping ratio increased by about 1% (from 3% to 4%) from low water level to almost full water level. Therefore, it is assumed that the damping ratio of the dam itself is smaller than the result shown in Fig. 16. On the other hand, it was identified that the damping ratio of the dam was 3% by a reproduction analysis of the behavior of the dam during an earthquake. The damping ratio identified by the reproduction analysis is slightly smaller than the evaluation result by the proposed method. It is presumed that the damping due to the reservoir water is taken into calculation naturally in the reproduction analysis where the dam and reservoir are treated as coupled system, and the damping ratio identified is that excluding the part due to the reservoir water. Therefore, it is considered that the evaluation results of the damping ratio of the dam by both methods basically agree.

Based on the above, it is considered that the proposed method can be applied to dams with strong three-dimensionality, and a practical method for evaluating damping ratios of dams. In the future, more data of dams will be used to improve the evaluation accuracy of the proposed method.

## 5. Conclusions

The following conclusions were obtained from this study.

1) A method has been proposed to calculate the damping ratio of a structure by decomposing the free vibration and the forced vibration from the earthquake record of the structure and applying the Logarithmic Decrement Method to the free vibration.
2) The method of applying the proposed method to real dams was studied. It was found that the damping ratio of a concrete arch dam obtained by applying the proposed method is 2-6%, independent of the acceleration amplitude when the maximum acceleration value of the foundation was less than about 50 $cm/s^2$. This result is almost consistent with the result identified by a reproduction analysis of the seismic behavior of the dam. This proved that the proposed method was practical as a method for evaluating damping ratios of dams.
3) For the existing dam used in the study, the contribution of reservoir water to damping ratio is estimated to be approximately 1% when water depth increases from 60 m to 100 m.

In the future, the applicability of the proposed method will be examined using more data, and it is expected the method will be improved to be more accurate and convenient.

## Acknowledgements

Many thanks to Mr. Hashimoto and Mr. Umehara of J-POWER Business Service Social Environment Department for their support during the study.



 

## References

[1] Cao Z., Kashiwayanagi M., Yoshida M., and Asaka H. (2017): Transfer function calculation method considering mutual interaction of vibration and its use in dam engineering, *Journal of Electric Power Civil Engineering*, No.390, 1-9

[2] Matsumoto N., Yasuda N., and Okubo M. (1986): Dynamic rigidity, damping and Poisson's ratio of coarse-grained materials. *Civil Engineering Journal*, No.28/7, 382-387 (in Japanese)

[3] Ueda M., Shiojiri H., Yokoi F., and Tsunekawa K. (1997): Damping constant obtained from arch dam earthquake observation records, *24th Proceedings of the JSCE Earthquake Engineering Symposium*, 825-828 (in Japanese)

[4] Sato N., Soda H., Ootagaki K. (2013): Estimation and application of dynamic and physical properties of existing dam embankment from measured earthquake records, *Dam Engineering*, No.321, 40-47 (in Japanese)

[5] Watanabe H., Ariga Y., and Cao Z. (2002): Earthquake resistance of a concrete gravity dam revaluated with 3-D nonlinear analysis, *Journal of JSCE*, No.696/I, 99-110 (in Japanese)

[6] Ohmachi, T. and Tahara, T. (2011): Nonlinear earthquake response characteristics of a central clay rockfill dam, *Soils and Foundations*, Vol.51, No.2, 227-238

[7] Timoshenko, S.: Vibration Problems in Enineering. D. Van Nostrand Company. Vol. 32,1929.

[8] JSCE (1986): *The Structural Mechanics Handbook*. 2nd edition.

[9] JSCE (1989): *Dynamic Analysis and Aseismic Design*, *Vol.3*., Gihodo, 1st edition.

[10] Matsumoto N., Yasuda N., and Cao Z. (2019): Long-term fluctuation in dynamic characteristics and propagating behaviors of seismic motion in a rockfill dam-foundation system. *Journal of JSCE*, Vol.7, 72-84



 